THE ASTROPHYSICAL JOURNAL, 346:424–434, 1989 November 1

MASS LOSS DURING NOVA OUTBURSTS FOR VARIOUS WHITE DWARF MASSES

MARIKO KATO
Department of Astronomy, Keio University

AND

IZUMI HACHISU
Department of Aeronautical Engineering, Kyoto University
Received 1988 April 22; accepted 1989 May 3

ABSTRACT

Optically thick winds have been observed in the decay phase of nova outbursts. The full decay phase of a nova is simulated by a sequence consisting of steady mass loss and static envelope models. In the sequence the hydrogen-rich envelope mass decreases from model to model as a result of wind mass loss and hydrogen burning. We have calculated six sequences for the white dwarf masses $M_{\rm WD} = 0.4$, 0.6, 0.7, 0.9, 1.0, and 1.2 $M_\odot$. It is found that optically thick wind occurs for $M_{\rm WD} > 0.8\ M_\odot$ if we assume solar chemical composition. The wind stops when the envelope mass is much reduced, mainly by the wind mass loss, and the photospheric radius $r_{\rm ph}$ becomes smaller than a certain value, which depends on the white dwarf mass. The wind stops at $\log T_{\rm ph} = 3.99$ ($r_{\rm ph} = 57.0\ R_\odot$) for $M_{\rm WD} = 0.9\ M_\odot$ and at $\log T_{\rm ph} = 5.21$ ($r_{\rm ph} = 0.283\ R_\odot$) for $M_{\rm WD} = 1.4\ M_\odot$, where $T_{\rm ph}$ is the photospheric temperature.

Empirical formulae relating the mass-loss rate and the mass of the hydrogen-rich envelope are obtained for three sequences: $M_{\rm WD} = 0.9$, 1.0, and 1.2 $M_\odot$. Using these formulae, we have estimated the evolutionary time scale of the decay phase and the amount of the mass lost from the system. The wind mass loss lasts 3.2 yr for $M_{\rm WD} = 1.0\ M_\odot$, and the ensuing static phase lasts 14 yr. The net accretion of helium matter depends both on the size of the Roche lobe and on the mass accretion rate. For $M_{\rm WD} > 1.0\ M_\odot$, it is less than 0.1 when the accretion rate is smaller than $\sim 10^{-10}\ M_\odot\ {\rm yr}^{-1}$ and about $\frac{1}{3}$ even when the accretion rate is as large as $1 \times 10^{-7}\ M_\odot\ {\rm yr}^{-1}$. The effect of the outer critical Roche lobe overflow significantly reduces this efficiency of accretion if its size is small enough.

If the white dwarf mass can grow to the Chandrasekhar limit during nova cycles, a Type Ia supernova explosion or accretion-induced collapse is expected to occur. In order for a white dwarf to grow from 1.0 to 1.38 $M_\odot$, the companion star should transfer more than 1.1 $M_\odot$ of matter to the white dwarf when the mass transfer rate is $1 \times 10^{-7}\ M_\odot\ {\rm yr}^{-1}$. It amounts to as much as 11 $M_\odot$ for $10^{-10}\ M_\odot\ {\rm yr}^{-1}$. We discuss the possibility of Type Ia supernova and neutron star formation induced by accretion in nova (recurrent nova) systems.

Subject headings: stars: binaries — stars: mass loss — stars: novae — stars: supernovae — stars: white dwarfs

I. INTRODUCTION

It has been suggested by many authors that neutron stars in low-mass binary pulsars are formed through the accretion-induced collapse of white dwarfs (e.g., van den Heuvel 1987 and references therein). The same mechanism is expected to occur in the progenitor systems of low-mass X-ray binaries (see, e.g., Taam and van den Heuvel 1986 and references therein). This mechanism is based on the assumption that accreting white dwarfs can grow to the Chandrasekhar limit. The accretion-induced collapse results from white dwarfs having initial masses larger than 1.2 $M_\odot$. If the initial mass of the white dwarf is smaller than 1.2 $M_\odot$, on the other hand, a Type Ia supernova explosion is expected to occur when the mass increases to the Chandrasekhar limit (e.g., Nomoto 1987*a*, *b*).

In these progenitor systems, white dwarfs accrete hydrogen-rich matter from the companion if the donors are normal stars. Then they will suffer many cycles of nova explosion when the mass transfer rate, $\dot{m}$, is smaller than $\sim 1 \times 10^{-7}\ M_\odot\ {\rm yr}^{-1}$ (e.g., Fujimoto 1982*b*; Iben 1982). One of the candidates for these progenitor systems is cataclysmic variables (e.g., McClintock and Rappaport 1985; Lipunov and Postnov 1985; Chanmugam and Brecher 1987). The mass transfer rate in cataclysmic variables falls into the range 10^{-11} to $10^{-7}\ M_\odot\ {\rm yr}^{-1}$ (e.g., Patterson 1984).

Once a strong nova explosion occurs, however, a significant part of the hydrogen-rich envelope mass is ejected from the system (see, e.g., Prialnik 1986). This implies that white dwarfs cannot grow to the Chandrasekhar limit when $\dot{m} \lesssim 10^{-9}\ M_\odot\ {\rm yr}^{-1}$ (e.g., Fujimoto 1982*a*, *b*; McDonald 1983). On the other hand, a weak nova explosion results from relatively high mass transfer rates such as $1 \times 10^{-7}\ M_\odot\ {\rm yr}^{-1}$. Therefore, it has been argued that a neutron star forms through the accretion-induced collapse of a white dwarf if the mass transfer rate is relatively high (e.g., Nomoto 1987*a*, *b*, for reviews of this type of discussion). In order to know whether accreting white dwarfs can grow to the Chandrasekhar limit or not, we must estimate how large an amount of the processed matter is accreted by the white dwarf during a relatively *weak* nova outburst.

A direct way to estimate the mass ejected is to simulate the time-dependent evolution of a nova outburst. Recently many hydrodynamical calculations have been done for relatively high accretion rates ($\dot{m} \gtrsim 10^{-8}\ M_\odot\ {\rm yr}^{-1}$) and the mass ejected during a nova is evaluated (Starrfield, Sparks, and Truran 1985, 1986; Truran *et al.* 1988; Livio, Prialnik, and Regev

1989; Kato, Saio, and Hachisu 1989). One characteristic common to these studies, except for Kato, Saio, and Hachisu's work (1989), is that model computations have been performed only for the first one or two cycles of a nova. It is, however, well known that the properties of the first flash depend largely on the initial condition. Therefore, the ejected mass calculated from the first shell flash is not guaranteed to be equal to the ejected mass after many cycles of flash. In this sense, any time-dependent calculations must be followed until successive shell flashes approach a limit cycle (see, e.g., Sugimoto and Miyaji 1981). Without accurate knowledge about such long-term evolutions of flash cycles, we cannot determine the correct value of the mass lost from the system, or, in other words, the efficiency of the mass accumulation (i.e., the ratio of the processed matter accreted by the white dwarf to the mass transferred from the companion during one cycle of a nova). Very recently, Kato, Saio, and Hachisu (1989) *did* perform such calculations and could obtain the accurate value of the mass accumulation ratio for helium-accreting white dwarfs. If we can choose an initial state which is close enough to the limit cycle, the model will reach the limit cycle shortly after a few flash cycles. Such a choice of the initial model is discussed in detail in § IV.

Another way to calculate the mass accumulation ratio is to use steady state solutions of wind. Among several works presented so far (Finzi and Wolf 1971; Ruggles and Bath 1979; Kato 1983; Kato and Hachisu 1988), Kato (1983) has first succeeded in constructing sequences of the decay phase of a nova. One important characteristic in her solutions is that the energy generation by nuclear burning is properly included. For this reason, both the mass-loss rate and the structure are uniquely determined without any other assumptions. Extending her sequence, Kato and Hachisu (1988) constructed a sequence for a full cycle of a nova on a 1.3 $M_\odot$ white dwarf. They demonstrated that wind mass loss occurs even in a very weak nova explosion for the mass accretion rate $\dot{m} = 1 \times 10^{-7}$ $M_\odot$ yr^{-1}. Their results showed that more than 70% of the accumulated matter is blown off once a weak nova explosion occurs.

Their results imply that a white dwarf probably cannot grow to the Chandrasekhar limit when the companion is a low-mass star, that is, for the progenitor systems of Type Ia supernovae, of low-mass X-ray binaries, or of long orbital period binary radio pulsars. Their work, however, treated only 1.3 $M_\odot$ white dwarfs and is insufficient to support the conclusion that white dwarfs cannot grow to the Chandrasekhar mass. In the present paper, we examine other white dwarf masses of $M_{\rm WD} = 0.4$, 0.6, 0.7, 0.9, 1.0, and 1.2 $M_\odot$, for which a decay phase of a nova is modeled by a sequence consisting of steady mass loss and static solutions. We also estimate the efficiency of mass accumulation, η, i.e., the ratio of the processed helium matter accreted by the white dwarf to the hydrogen-rich matter transferred from the companion star.

The numerical method and the various physical assumptions are essentially the same as those in our previous paper (Kato and Hachisu 1988, hereafter Paper I). The basic equations and other assumptions are the same as Kato's (1983) unless we specifically state otherwise. In § II we describe the numerical solutions both for the steady mass loss and for the static cases. In § III the efficiency of mass accumulation is estimated including the effect of the outer critical Roche lobe overflow. In this paper, we assume the solar abundance of the hydrogen-rich envelope. This assumption is often violated in classical nova systems. So, the influence of the chemical composition on the accumulation ratio is discussed in § IV. To check our assumption of the steady state approach, we compare our solutions with other time-dependent calculations in § V. Also, here we discuss the influence of our results on the scenario of Type Ia supernovae, and on the formation mechanism of neutron stars.

II. MASS-LOSS SOLUTIONS OF A NOVA OUTBURST

First we will show a schematic diagram of the evolutionary course of a nova outburst (see Fig. 1) and briefly explain the important epochs of the nova phenomenon. Before the onset of a nova, the accreting white dwarf stays at point A in Figure 1. When the envelope mass exceeds a critical value, unstable hydrogen burning ignites to trigger a nova outburst. The star brightens up and goes up in the H-R diagram. The hydrogen-rich envelope absorbs energy generated by nuclear reactions and expands on a large scale; the star goes redward. Mass loss occurs at point B owing to stellar wind or to the Roche lobe overflow, which depends on the binary parameters, as will be explained below. At point C the envelope reaches a thermal equilibrium: the energy generated by nuclear burning balances the energy loss. After the maximum expansion of the photospheric radius, the star moves blueward, decreasing its envelope mass. A large amount of the hydrogen-rich envelope mass has been lost from the system when the mass loss stops at point D. After point D, the hydrogen-rich envelope mass gradually decreases in time as a result of hydrogen burning and the star goes blueward. The nuclear burning ceases at point E and the star gradually cools down to point A.

Such an evolutionary path of a nova can be followed by a sequence consisting of static solutions and steady mass-loss solutions. In Paper I we computed a complete nova cycle for a 1.3 $M_\odot$ white dwarf and showed that the rising phase (from

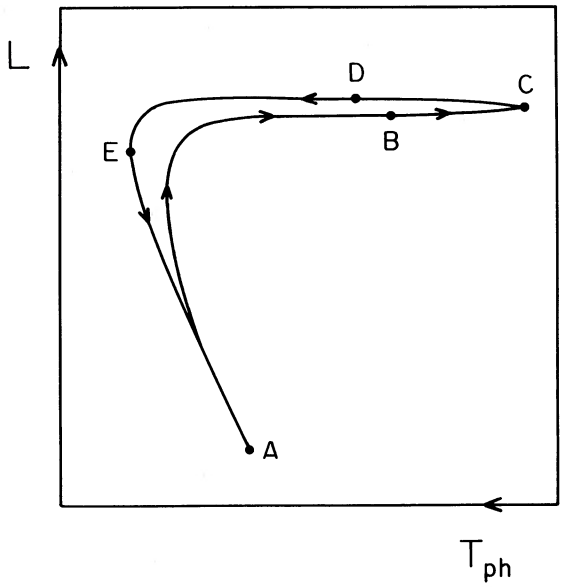

FIG. 1.—A schematic H-R diagram for an evolutionary course of a nova. An accreting white dwarf stays at point A before the onset of the hydrogen shell flash. When the envelope mass reaches a critical value, unstable hydrogen shell burning ignites to trigger a nova. The star brightens. The envelope absorbs energy generated by nuclear burning and expands greatly. Mass loss starts at point B. After the photospheric radius reaches the maximum value at point C, the envelope reaches thermal equilibrium. The mass of the hydrogen-rich envelope decreases in time as a result of both mass loss and nuclear burning. The mass loss stops at point D. Nuclear burning ceases at point E.

point A to point C in Fig. 1) depends on the ignition mass but the decay phase (from point C to point E) is uniquely identified almost independent of the ignition mass, because the decay phase is in thermal equilibrium. Since the effective mass accumulation ratio, η, and the duration of a nova are determined mainly by this later phase, we present sequences only for the decay phase of a nova, assuming various masses of white dwarf. As mentioned in § I, we use the same assumptions and the same numerical techniques as in Paper I (see also Kato 1983 for the basic equations). The envelope is assumed to have a uniform chemical composition $(X, Y, Z) = (0.73, 0.25, 0.02)$ by weight for hydrogen (X), helium (Y), and heavy elements (Z), respectively. We will discuss the influence of the chemical composition on the solutions in § IV. The radii of the white dwarfs are assumed to be the Chandrasekhar radius with the mean molecular weight per electron being $\mu_e = 2$ (see § V*b* for more detailed description).

Figure 2 depicts evolutionary tracks of the decay phases of a nova for eight different white dwarf masses (the sequence of a 1.3 $M_\odot$ white dwarf is taken from Paper I; only the static part of the sequence is added for a 1.4 $M_\odot$ white dwarf). Attached numbers denote the white dwarf masses in solar mass units. Mass-loss solutions are plotted discretely by crosses or by other symbols. Physical properties of the wind mass-loss solutions for a 1.3 $M_\odot$ white dwarf have already been described in Kato (1983). Short vertical bars denote the points at which the steady wind terminates (Kato 1985). We have searched for wind solutions in the region of $\log T_{\rm ph} > 3.8$ and found that optically thick winds occur only for massive white dwarfs ($M_{\rm WD} \gtrsim 0.9\ M_\odot$). Filled circles denote the extinction points of hydrogen burning (point E in Fig. 1).

The luminosity of the wind mass-loss solutions drops largely redward in the H-R diagram (Fig. 2) and increases again. The reason is as follows: the nuclear energy generation at the bottom of the hydrogen-rich envelope is almost constant in time, or, in our terminology, from model to model, but a part of the diffusive energy is consumed in pushing the matter up against gravity. This is the reason why the luminosity decreases in the red side of the H-R diagram. If the wind is very strong, however, there exist superadiabatic regions in the ionization zones. The diffusive luminosity decreases outward in the inner part of the envelope to push the matter up, but it increases in the outer part of the envelope because the internal energy is converted into diffusive luminosity in the superadiabatic regions. It seems that there exists a forbidden region in the H-R diagram for mass-loss solutions. This is similar to Hayashi's forbidden region, but the physical meaning is different. (The position of Hayashi track is rather redward to our forbidden region).

The envelope mass at each epoch is tabulated in Table 1. The last column of the table lists the ignition masses for a limiting case of high accretion rates, i.e., the ignition mass for the accretion rate of $1 \times 10^{-7}\ M_\odot\ {\rm yr}^{-1}$ (taken from Nariai and Nomoto 1979). The faster the mass transfer, the weaker the nova outbursts and the smaller the ignition mass. When the accretion rate is higher than $2 \times 10^{-7}\ M_\odot\ {\rm yr}^{-1}$, no nova explosions occur because the hydrogen nuclear burning is stable. Therefore, we will refer to the ignition mass at the accretion rate of $1 \times 10^{-7}\ M_\odot\ {\rm yr}^{-1}$ as the minimum ignition mass. In all cases of the massive white dwarfs ($M_{\rm WD} \geq 0.9\ M_\odot$) the minimum ignition mass is larger than the envelope mass at the point where the wind has just stopped (fifth column in Table 1). This indicates that wind mass loss necessarily occurs even in the weakest nova when $M_{\rm WD} \geq 0.9\ M_\odot$. The reason why the wind mass loss does not occur in the relatively less massive white dwarfs is as follows: the wind is accelerated by the radiation pressure gradient. In the massive white dwarfs, the radiation pressure gradient is strong enough compared with gravity because its luminosity is very close to the Eddington limit. In the less massive white dwarfs, on the other hand, the luminosity cannot reach the Eddington limit but is sub-Eddington throughout the envelope. As a result, the radiation-driven acceleration does not work effectively.

The mass-loss rate in the wind phase, $\dot{M}$ (<0), is plotted in Figure 3 against the hydrogen-rich envelope mass ΔM. The mass-loss rate is large when the photospheric temperature is

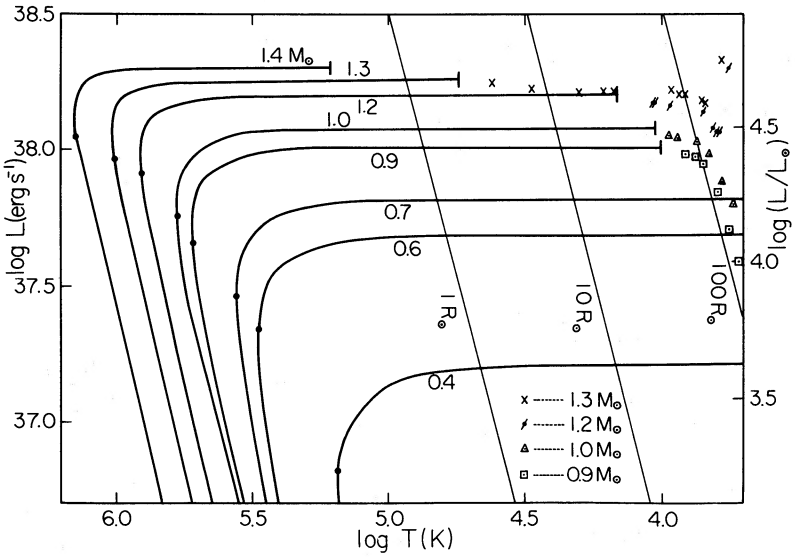

FIG. 2.—Evolutionary courses of novae after the maximum expansion of the photospheric radius. Solutions of optically thick winds are discretely denoted by crosses or by the other symbols, which are explained in the figure. Static solutions are plotted in thick solid lines. Short vertical bars denote the solutions at which the wind just stops. The extinction point of hydrogen burning is denoted by filled circles. Thin solid lines are the constant-radius lines of 1, 10, and 100 $R_\odot$.

TABLE 1

ENVELOPE MASSES[a]

M_{WD}	Point E ΔM(E)	$r_{ph} = 1\ R_\odot$	$r_{ph} = 10\ R_\odot$	Point D ΔM(D)	ΔM_i[b]
0.4.....	8.21(−5)[c]	1.89(−4)	2.46(−4)	...	4.4(−4)
0.6.....	1.71(−5)	5.53(−5)	6.98(−5)	...	1.3(−4)
0.7.....	1.02(−5)	3.51(−5)	4.30(−5)	...	8.5(−5)
0.9.....	3.06(−6)	1.05(−5)	1.17(−5)	1.29(−5)	3.4(−5)
1.0.....	1.89(−6)	6.09(−6)	6.76(−6)	7.47(−6)	2.2(−5)
1.2.....	5.65(−7)	1.43(−6)	1.50(−6)	1.71(−6)	6.6(−6)
1.3.....	1.92(−7)	3.72(−7)	...	3.74(−7)	2.5(−6)
1.4.....	3.91(−8)	...	...	5.61(−8)	1.8(−7)

[a] Masses are measured in solar mass units.
[b] Minimum ignition masses are taken from Nariai and Nomoto 1979.
[c] 8.21(−5) means 8.21×10^{-5}.

low. It becomes smaller as the star moves blueward in the H-R diagram. We made up, in Paper I, an empirical formula for the mass-loss rate in the decay phase for a 1.3 $M_\odot$ white dwarf: the mass-loss rate $\dot{M}$ is proportional to $(\Delta M)^{1.5}$. This formula is plotted by a thin solid line in Figure 3. For the other white dwarf masses, the power index is about 1.5 for large envelope masses, but it is much steeper before the wind stops, that is, when the envelope mass is small. Therefore, our empirical formula may consist of two different power indices as follows: for our 1.2 $M_\odot$ white dwarf,

$$\log |\dot{M}| = \begin{cases} 1.45 \log \Delta M + 3.00 & \text{for } \log \Delta M \geq -4.3\ , \\ 1.89 \log \Delta M + 4.89 & \text{for } \log \Delta M < -4.3\ , \end{cases} \quad (1)$$

where the wind mass-loss rate is in units of $M_\odot\ \mathrm{yr}^{-1}$ and the envelope mass is also in solar mass units ($M_\odot$). This formula holds for $-5.3 \leq \log \Delta M \leq -3.4$, which corresponds to the range of the mass-loss rate $-5.1 \leq \log |\dot{M}| \leq -1.95$. For our 1.0 $M_\odot$ white dwarf,

$$\log |\dot{M}| = \begin{cases} 1.55 \log \Delta M + 2.93 & \text{for } \log \Delta M \geq -4.0\ , \\ 2.15 \log \Delta M + 5.31 & \text{for } \log \Delta M < -4.0\ . \end{cases} \quad (2)$$

This formula holds for $-4.80 \leq \log \Delta M \leq -3.32$, which corresponds to the mass-loss rate $-5.04 \leq \log |\dot{M}| \leq -2.22$. For our 0.9 $M_\odot$ white dwarf,

$$\log |\dot{M}| = \begin{cases} 1.54 \log \Delta M + 2.54 & \text{for } \log \Delta M \geq -4.15\ , \\ 2.74 \log \Delta M + 7.56 & \text{for } \log \Delta M < -4.15\ . \end{cases} \quad (3)$$

This holds for $-4.6 \leq \log \Delta M \leq -2.78$, which corresponds to the mass-loss rate $-5.0 \leq \log |\dot{M}| \leq -1.68$. These formulae are plotted in Figure 3 by thick solid lines.

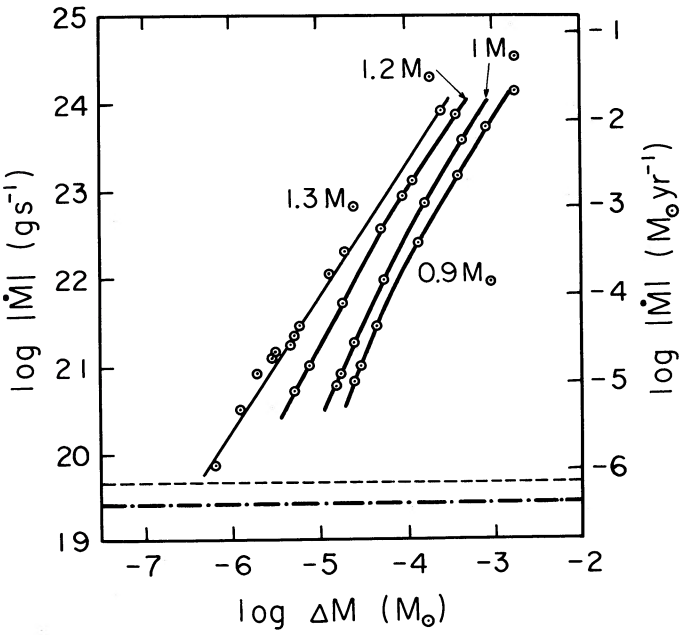

FIG. 3.—Wind mass-loss rate, $\dot{M}$, of each solution, plotted against the envelope mass ΔM. The thin solid line denotes the empirical formula of a 1.3 $M_\odot$ white dwarf. Thick solid lines correspond to 1.2, 1.0, and 0.9 $M_\odot$ white dwarfs. Dashed and dot-dash lines denote the decreasing rates of the hydrogen-rich envelope due to nuclear burning for 1.3 and 0.9 $M_\odot$, respectively.

The evolutionary time scale of a nova outburst can be estimated by using the empirical formulae of wind mass-loss rate. To do it, we divide the decay phase of a nova into two parts, i.e., the wind phase and the ensuing static nuclear burning phase. In the wind phase the envelope mass decreases owing to both wind mass loss and hydrogen burning. The decreasing rate due to nuclear burning is also plotted in Figure 3: a dashed line for 1.3 $M_\odot$ and a dash-dot line for 0.9 $M_\odot$. This rate is much smaller than that due to wind mass loss. Therefore, we can neglect the effects of nuclear burning when we estimate the decreasing rate of the hydrogen-rich envelope mass during the wind phase. The duration of the wind phase, t_{ML}, can be estimated from

$$t_{ML} = \int_{\Delta M}^{\Delta M(D)} \frac{dM}{\dot{M}}\ . \quad (4)$$

The upper bound of the integration, ΔM(D), is the envelope mass at point D (cease point of the wind). The value of ΔM(D) is listed in the fifth column of Table 1. The lower bound of the integration, ΔM, can be replaced with the initial envelope mass ΔM_i, if the size of the outer critical Roche lobe is sufficiently large. If the Roche lobe is small enough, however, the duration may shorten because matter outside the outer critical Roche lobe is quickly lost from the system, as will be explained in the next section. We summarize in Table 2 the duration of the wind phase for two cases: a relatively low accretion rate ($\dot{m} = 1 \times 10^{-10}\ M_\odot\ \mathrm{yr}^{-1}$) and a high mass accretion rate ($\dot{m} = 1 \times 10^{-7}\ M_\odot\ \mathrm{yr}^{-1}$). Here we use the relation between the mass accretion rate and the ignition mass calculated by Nariai and Nomoto (1979).

After the wind stops the envelope mass decreases as a result

TABLE 2

EVOLUTIONARY TIME SCALE OF NOVAE

M_{WD} ($M_\odot$)	t_{AD}[a] (yr) ($\dot{m} = 10^{-10}$ $M_\odot$ yr^{-1})	t_{AD} (yr) ($\dot{m} = 10^{-7}$ $M_\odot$ yr^{-1})	t_{D10}[b] (yr)	t_{101}[c] (yr)	t_{1E}[d] (yr)
1.2.....	2.0	1.5	0.36	0.14	1.6
1.0.....	3.2	2.4	1.6	1.6	11
0.9.....	5.2	4.1	3.2	4.0	22
0.7.....	...	...	...	34	120
0.6.....	...	...	...	78	250
0.4.....	...	...	...	980	2300

[a] Time from the ignition point (point A) to the point at which the wind just stops (point D).

[b] Time from point D to the point where the photospheric radius, r_{ph}, decreases to 10 $R_\odot$.

[c] Time from the point where $r_{ph} = 10\ R_\odot$ to the point where $r_{ph} = 1\ R_\odot$.

[d] Time from the point where $r_{ph} = 1\ R_\odot$ to the extinction point of nuclear burning (point E).

of hydrogen burning. The duration of the static phase (from point D to point E) is calculated from

$$t_{ST} = \epsilon_H X \int_{\Delta M(E)}^{\Delta M(D)} \frac{dM}{L}, \quad (5)$$

where ϵ_H and L are the energy generation rate per unit mass by hydrogen burning, and the luminosity, respectively. In Table 2 we also tabulate the time scale in which the star moves from the wind termination point (point D) to the point at which the photospheric radius, r_{ph}, reaches 10 $R_\odot$, the time scale from $r_{ph} = 10\ R_\odot$ to $r_{ph} = 1.0\ R_\odot$, and the time scale from $r_{ph} = 1.0\ R_\odot$ to the extinction point of nuclear burning (point E).

III. MASS ACCUMULATION RATIO

During a nova outburst a significant part of the initial envelope mass is blown off. In this section we will estimate the amount of the processed matter (helium) accreted by the white dwarf during one nova cycle. First we consider the mass loss due only to wind. This corresponds to the case of very large Roche lobe size ($\gtrsim 100\ R_\odot$). Next we estimate the mass loss due to the outer critical Roche lobe overflow.

When the Roche lobe is very large, wind mass loss is the main mechanism which reduces the mass of the hydrogen-rich envelope for $M_{WD} \geq 0.9\ M_\odot$. The nuclear burning always converts hydrogen into helium throughout the mass-loss phase and the static phase. We divide the helium mass accreted by the white dwarf into two parts:

$$\Delta M_{He} = \Delta M_{He,\,CD} + \Delta M_{He,\,DE}, \quad (6)$$

where $\Delta M_{He,\,CD}$ and $\Delta M_{He,\,DE}$ are the helium masses accreted by the white dwarf during the wind and the static phase, respectively. We do not include the helium mass processed in the previous phase (from point A to point C through point B in Fig. 1), because the convection develops widely at the first phase of the nova and the processed matter is mixed into the upper part of the envelope (Nariai, Nomoto, and Sugimoto 1980; Prialnik 1986), which is lost later from the system by the wind. The helium mass during the wind phase is calculated from

$$\Delta M_{He,\,CD} = t_{ML} L_n / \epsilon_H X. \quad (7)$$

where L_n is the energy generation rate by hydrogen burning. The amount of helium processed in the static phase is calculated from the difference between the masses of two static solutions, i.e.,

$$\Delta M_{He,\,DE} = \Delta M(D) - \Delta M(E). \quad (8)$$

Now we define the mass accumulation ratio, η, i.e., the ratio of the helium mass accreted by the white dwarf to the transferred hydrogen-rich matter during one nova cycle, as follows:

$$\eta = \Delta M_{He} / [\Delta M_i - \Delta M(E)]. \quad (9)$$

It should be noted here that the envelope mass at the extinction point of nuclear burning (point E), $\Delta M(E)$, remains unprocessed and will suffer the next outburst. Figure 4 depicts the mass accumulation ratio η plotted against the mass transfer rate $\dot{m}$ (>0) from the companion. The accumulation ratio is large for high accretion rate mainly because the ignition mass is small.

If the size of the outer critical Roche lobe is small enough, the Roche lobe overflow comes into effect. Matter outside the outer critical Roche lobe will certainly be lost from the system if the envelope expands greatly beyond the outer critical Roche lobe. Sawada, Hachisu, and Matsuda (1984) simulated such a gas flow in contact binaries. They showed that the matter outside the outer critical Roche lobe is getting angular momentum from the binary potential and moving outward. The flow pattern shows that the outward velocity is about one-tenth of the orbital velocity of the binary. Since the time scale of the outer critical Roche lobe overflow is a dynamical one, we consider that the mass loss from the Roche lobe occurs very quickly compared with the duration of the later static phase, t_{ST}, and no significant amount of helium matter is accreted by the white dwarf during this Roche lobe overflow phase.

The mass accumulation ratio for this case is obtained from equations (8) and (9) by replacing the envelope mass $\Delta M(D)$ with the mass of the static model having radius equal to the Roche lobe. The accumulation ratio is plotted in Figures 5 and

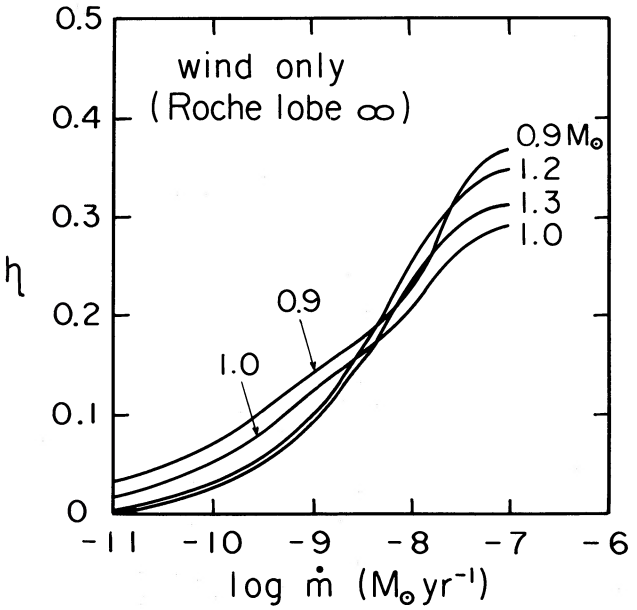

FIG. 4.—Ratio η of the helium matter accumulated on the white dwarf to the mass transferred from the companion star before the ignition, plotted against the mass accretion rate. The effect of the outer critical Roche lobe overflow is neglected.

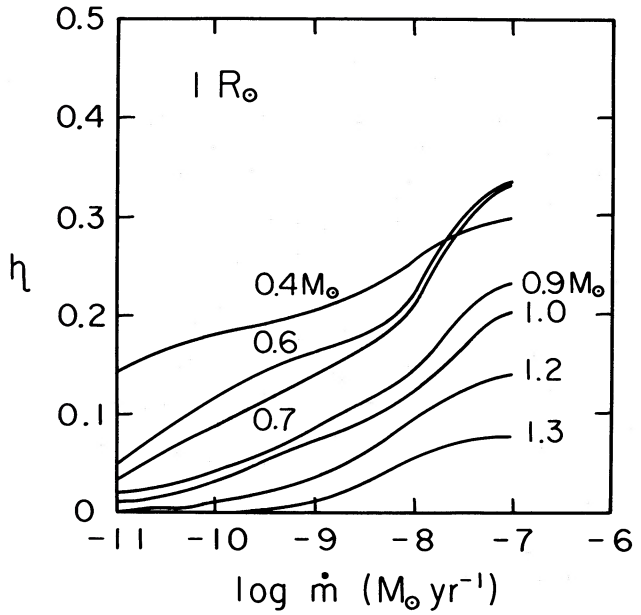

FIG. 5.—Same as Fig. 4, but for the case in which the size of the outer critical Roche lobe is assumed to be 1 $R_\odot$.

6 against the mass transfer rate for two different Roche lobe sizes, i.e., 1.0 $R_\odot$ and 10 $R_\odot$, respectively.

From Figures 4, 5, and 6, we can estimate how much mass is needed for a white dwarf to grow from 1.0 to 1.38 $M_\odot$, that is, $\sum \Delta M/\eta$ under the condition $\sum \Delta M = 0.38\ M_\odot$. In Table 3 the mass required is listed for various parameters. It is as large as 1.1 $M_\odot$ even in the case of high mass accretion rate and very large Roche lobe size. This result implies that a white dwarf cannot grow from 1.0 to 1.38 $M_\odot$ if the companion star is smaller than 1.1 $M_\odot$ and the mass transfer rate is lower than $\dot{m} = 1 \times 10^{-7}\ M_\odot\ \mathrm{yr}^{-1}$.

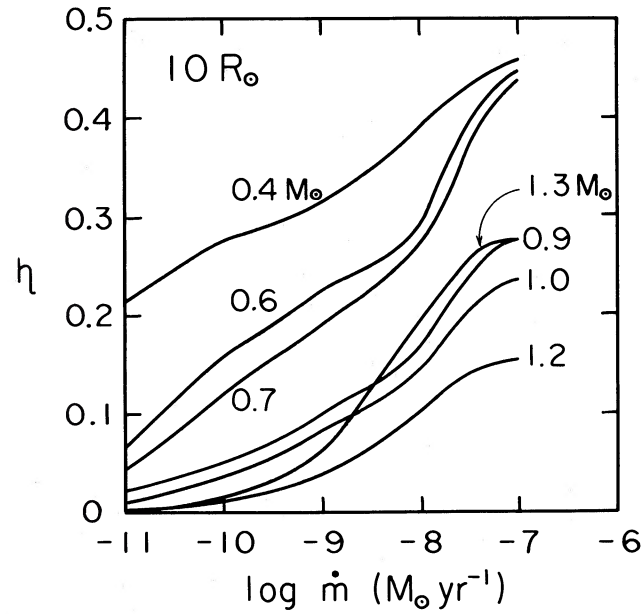

FIG. 6.—Same as Fig. 4, but for the case in which the Roche lobe is 10 $R_\odot$

TABLE 3

MASS REQUIRED FOR A 1 $M_\odot$ WHITE DWARF TO GROW TO 1.38 $M_\odot$

Mass Transfer Rate log $\dot{m}$ ($M_\odot$ yr^{-1})	Roche Lobe Size ($R_\odot$)	Required Mass ($M_\odot$)
−7	1	2.8
−7	10	1.9
−7	∞	1.1
−8	1	4.7
−8	10	2.7
−8	∞	1.7
−10	∞	11.3

IV. CHEMICAL COMPOSITION

Heavy-element enhancement is often observed in nova ejecta. In this section we discuss the influence of the chemical composition differing from solar abundance on our results.

Both the steady mass loss and static solutions described in § II depend weakly on the chemical composition. The chemical composition affects the envelope structure through mean molecular weight, opacity, and nuclear burning rate. The effect of the nuclear burning rate is rather small in the decay phase compared with that in the rising phase of the nova. In the beginning of the shell flash the enhancement of CNO elements increases the nuclear burning rate and leads to a much more violent explosion than in the case of solar abundance (e.g., MacDonald 1983). Therefore, the rising phase is strongly affected by the enhancement of CNO elements. It has been believed that such enhancement of the heavy element causes a fast nova. However, we believe that the decay phase of the nova depends weakly on the enhancement of heavy elements because the nuclear burning is stable.

In order to check the influence of the chemical composition on the envelope structure, we have calculated static solutions for various compositions. For 1.3 $M_\odot$ white dwarf, we obtained static solutions at point D in Figure 1 (where the wind mass loss has just stopped). For 1.0 and 0.6 $M_\odot$ white dwarfs, models having 1.0 $R_\odot$ are calculated to see how much η is changed.

a) Helium Enhancement

First, we examine the influence of helium enhancement. The heavy elements are assumed to have solar abundances throughout this subsection. For a 1.3 $M_\odot$ white dwarf, we have, in the previous sections, shown a model at point D assuming the chemical composition (X, Y, Z) = (0.73, 0.25, 0.02). The envelope mass is $\Delta M(\mathrm{D}) = 3.74 \times 10^{-7}\ M_\odot$. If we increase the helium content to (0.63, 0.35, 0.02), $\Delta M(\mathrm{D}) = 3.61 \times 10^{-7}\ M_\odot$. This value of helium enhancement is estimated from the hydrogen burning during the rising phase of the nova. In order for the envelope to expand on a large scale, the total nuclear energy generated by hydrogen burning is almost equal to the gravitational energy of the envelope on the white dwarf surface. Using this relation, we can estimate the total amount of the processed matter to lift the envelope up against the gravity. The convection at the rising phase mixes it with the upper part of the envelope. Therefore we use the averaged value of the helium content throughout the envelope. Then the helium content is increased to $Y = 0.35$ for a 1.3 $M_\odot$ white dwarf.

Recently helium enhancement has been observed in U Sco (Barlow *et al.* 1981; Williams *et al.* 1981). The number ratio of

helium to hydrogen is about He/H = 2. For such a hydrogen-deficient model of (0.109, 0.871, 0.02), $\Delta M(\mathrm{D}) = 3.76 \times 10^{-7}$ $M_\odot$. The differences among these envelope masses are very small compared with the difference in envelope mass between points D and E, which is important to estimate the mass accumulation ratio.

One mass-loss solution is also calculated for the case of (0.63, 0.35, 0.02). The mass-loss rate is 2.15×10^{21} g s^{-1} when the envelope mass is 4.46×10^{-6} $M_\odot$. This mass-loss rate is very close to the line in Figure 3. For the case of (0.48, 0.5, 0.02) the mass-loss rate is 3.33×10^{21}g s^{-1} at the envelope mass of 5.50×10^{-6} $M_\odot$. This rate is a little bit above the line because of the effect of the ionization zone. (This reason is the same as for the solutions around $|\dot{M}| = 10^{21}$ g s^{-1} in Fig. 3.) The wind solutions just before the wind stops is very similar to the static solutions at point D. Therefore, we may conclude that the envelope structures and the wind mass-loss rates of a 1.3 $M_\odot$ white dwarf are hardly affected by helium enhancement.

We have also computed the envelope masses having $r_{\rm ph} = 1.0$ $R_\odot$ on a 1.0 $M_\odot$ white dwarf. For the case of (0.73, 0.25, 0.02), the envelope mass is 6.09×10^{-6} $M_\odot$. It is 5.58×10^{-6} $M_\odot$ for the case of (0.5, 0.48, 0.02). A very low hydrogen content of (0.109, 0.871, 0.02) produces $\Delta M = 5.23 \times 10^{-6}$ $M_\odot$. Thus, the envelope mass depends weakly on the helium content. So we have further calculated solutions at point E in order to obtain the mass accumulation ratio (see § IVc). The envelope mass at point E is $\Delta M(\mathrm{E}) = 1.93 \times 10^{-6}$ $M_\odot$ for $X = 0.5$, and $\Delta M(\mathrm{E}) = 2.46 \times 10^{-6}$ $M_\odot$ for $X = 0.109$. Although we searched for the solutions corresponding to point D, we could not obtain them, at least for the region of $\log T_{\rm ph} > 4.0$. Therefore, we may conclude that the mass loss does not occur, at least for $X \leq 0.5$ and $\log T_{\rm ph} > 4.0$.

For a 0.6 $M_\odot$ white dwarf, the envelope mass of the model having $r_{\rm ph} = 1.0$ $R_\odot$ is 5.53×10^{-5} $M_\odot$ for (0.73, 0.25, 0.02), 5.31×10^{-5} $M_\odot$ for (0.5, 0.48, 0.02) and 5.50×10^{-5} $M_\odot$ for (0.109, 0.781, 0.02). The differences among these envelope masses are very small. Therefore, we may consider that the helium enhancement hardly affects the envelope mass and the envelope structure for 0.6 $M_\odot$ white dwarfs.

b) *Heavy-Element Enhancement*

Next, we discuss the effect of heavy-element (Z) enhancement. The envelope mass is sensitive to the heavy-element content. We calculate at first the solutions at point D for a 1.3 $M_\odot$ white dwarf. As we are increasing the heavy-element content Z, the envelope mass decreases to $\Delta M(\mathrm{D}) = 3.35 \times 10^{-7}$ $M_\odot$ for (0.73, 0.24, 0.03), and to 3.06×10^{-7} $M_\odot$ for (0.72, 0.24, 0.04). For the case of (0.53, 0.43, 0.04), which is supposed to be the composition of the slow nova RR Pic (Truran and Livio 1986), $\Delta M(\mathrm{D}) = 2.89 \times 10^{-7}$ $M_\odot$. For (0.015, 0.7, 0.285), the surface composition of Prialnik's (1986) fast nova model at which the luminosity begins to decline, $\Delta M(\mathrm{D}) = 2.02 \times 10^{-7}$ $M_\odot$. For the composition of the fast nova V1500 Cyg (Truran and Livio 1986), i.e., (0.49, 0.21, 0.3), $\Delta M(\mathrm{D}) = 1.76 \times 10^{-7}$ $M_\odot$. It is 1.37×10^{-7} $M_\odot$ for (0.45, 0.15, 0.4), 1.18×10^{-7} $M_\odot$ for (0.15, 0.05, 0.8), and 1.59×10^{-7} $M_\odot$ for (0.05, 0.15, 0.8). Therefore, the enhanced heavy element reduces the envelope mass by a factor of 2–3. This tendency can be extended for metal-deficient models such as (0.73, 0.269, 0.001). Then, $\Delta M(\mathrm{D}) = 8.32 \times 10^{-7}$ $M_\odot$. The envelope mass is twice as large as the solar abundance models.

Before we go to less massive white dwarfs, we explain a general tendency of the wind mass-loss solutions. The wind continues until the envelope mass is much more reduced if Z is increased. To see such a tendency, we increase Z and decrease X. Then the opacity decreases and, as a result, the luminosity goes up. Although the Eddington luminosity also goes up, the ratio of the total luminosity to the Eddington luminosity becomes larger because the increase in the total luminosity exceeds that in the Eddington luminosity. For this reason, the envelope mass at point D is much smaller in metal-enhanced models than in the solar abundance models.

We have calculated the envelope masses for a 1.0 $M_\odot$ white dwarf. For the case of (0.45, 0.15, 0.4), the mass of the envelope having $r_{\rm ph} = 1.0$ $R_\odot$ is 2.58×10^{-6} $M_\odot$. If we decrease X to (0.1, 0.5, 0.4), the wind mass loss stops at $r_{\rm ph} = 0.87$ $R_\odot$ ($\log T_{\rm ph} = 4.98$), where the envelope mass is 2.24×10^{-6} $M_\odot$. For the case of (0.053, 0.085, 0.862), the composition of the fast nova V1370 Aql (Truran and Livio 1986), the wind stops at $r_{\rm ph} = 0.229$ $R_\odot$ ($\log T_{\rm ph} = 5.273$), where the envelope mass is 1.66×10^{-6} $M_\odot$. For the small Z of (0.73, 0.269, 0.001), on the other hand, the envelope mass is increased to 1.38×10^{-5} $M_\odot$ for the model having $r_{\rm ph} = 1.0$ $R_\odot$.

For 0.6 $M_\odot$ white dwarf model, we have no wind solutions for the solar abundance, i.e., (0.73, 0.25, 0.02). If we increase Z to (0.45, 0.15, 0.4), wind occurs. It stops at $r_{\rm ph} = 16.13$ $R_\odot$ ($\log T_{\rm ph} = 4.229$), where the envelope mass is 3.25×10^{-5} $M_\odot$. If we decrease X to (0.1, 0.5, 0.4), the envelope mass is 2.50×10^{-5} $M_\odot$ for the solution at point D, i.e., $r_{\rm ph} = 3.58$ $R_\odot$ and $\log T_{\rm ph} = 4.598$. If we further increase Z to (0.053, 0.085, 0.862), the envelope mass is $\Delta M(\mathrm{D}) = 1.52 \times 10^{-5}$ $M_\odot$ at point D, where $r_{\rm ph} = 0.735$ $R_\odot$ and $\log T_{\rm ph} = 4.95$. The small Z of (0.73, 0.269, 0.001) increases the envelope mass up to 1.24×10^{-4} $M_\odot$ at $r_{\rm ph} = 1.0$ $R_\odot$.

To summarize, among all of our results here we may conclude that the envelope mass is much reduced by the increase in heavy elements (up to a factor of 2–3) but is little affected by the enhancement of helium content. This can be explained as follows: As mentioned above, the chemical composition affects the envelope mass through the mean molecular weight, nuclear burning rate, and opacity. The decrease in the hydrogen content leads to the increase in the mean molecular weight. This effect increases the density through the equation of state. As a result, the envelope mass increases. On the other hand, the decrease in the hydrogen content reduces the opacity. Then the total luminosity increases and the envelope mass decreases. The dependence of the envelope mass on the chemical composition is determined by the balance of these two effects. If we increase the helium content with Z unchanged, these two effects just balance each other. If we increase Z with Y fixed, these two effects cannot be balanced. This is because the nuclear burning rate in the CNO cycle, which is proportional to the product of X and Z, increases the luminosity without an increase in the density. Therefore, the envelope mass must decrease because the reduction of the pressure coming from the increase in the mean molecular weight can support only the less massive envelope.

c) *Influence of Helium Enhancement on the Accumulation Ratio*

We have already shown that the envelope mass is hardly affected by the enhancement of helium content. So we may assume that the ignition mass for such helium-enhanced matter is also little affected by the enhancement of helium. For the case of heavy-element enhancement, however, the ignition mass probably changes by a factor of 2–3 corresponding to the

change of the envelope mass. Therefore, we cannot correctly estimate the accumulation ratio until the ignition mass is obtained. For this reason, we will, in this subsection, estimate the mass accumulation ratio only for the case of helium enhancement.

If the helium content Y is increased with Z fixed, the elapsed time of the static phase becomes shorter, corresponding to equation (5). The star moves faster from point D to point E in Figure 1 than for the solar abundance. On the other hand, the elapsed time of the wind phase is probably not affected so much because the envelope mass-decreasing rate due to wind mass loss is much larger than that due to nuclear burning unless X is as small as 0.1. The processed mass accreted by the white dwarf during the static phase is, however, unchanged because it is calculated from equation (8). The mass accumulated during the wind phase is increased by a factor of $0.73/X$ from equation (7) if the elapsed time of the wind phase is not changed. Therefore, we can easily estimate the mass accumulation ratio for various values of X in equation (7).

i) 1.3 $M_\odot$

First, we examine the mass accumulation ratio assuming a very large Roche lobe size. When the composition is assumed to be (0.63, 0.35, 0.02), $\eta = 0.35$, 0.28, and 0.10 for $\dot{m} = 1 \times 10^{-7}$, 1×10^{-8}, and 1×10^{-9} $M_\odot$ yr^{-1}, respectively. The corresponding values are 0.31, 0.25, and 0.091 for the solar composition (0.73, 0.25, 0.02). Thus, the accumulation ratio increases only by 10%. If we reduce X to 0.1089, the accumulation ratio is close to unity. For example, our simple estimate mentioned above gives values larger than unity for $\dot{m} = 1 \times 10^{-7}$ and 1×10^{-8} $M_\odot$ yr^{-1}. (For $\dot{m} = 1 \times 10^{-9}$ $M_\odot$ yr^{-1}, $\eta = 0.50$.) When X is as small as 0.1 or less, the energy generated by hydrogen nuclear burning is almost equal to or smaller than the gravitational energy of the envelope for a 1.3 $M_\odot$ white dwarf. Therefore, only a very small part of the envelope mass would be ejected even if the wind mass loss occurs. In such a case, we may consider that almost all of the envelope mass can be accreted by the white dwarf. (We cannot correctly estimate the value from eqs. [6]–[9] under the assumption that the elapsed time of the wind phase, $t_{\rm ML}$, is not changed. This assumption is not correct when the time scale of the wind mass loss is comparable to that of the nuclear burning.) To calculate the correct value of the accumulation ratio for such cases, we must follow time-dependent evolutions of the hydrogen shell flash and examine how much the envelope expands. If the radius exceeds the value at point D, wind mass loss will certainly occur (Kato, Saio, and Hachisu 1989). Then we integrate equation (4) correctly, including both of the mass-decreasing rates (i.e., replacing $\dot{M}$ with $-|\dot{M}| - \dot{M}_{\rm nuc}$, where $\dot{M}_{\rm nuc}$ is the mass-decreasing rate due to hydrogen burning) as done by Kato, Saio, and Hachisu (1989) for helium novae (helium shell flashes). This value will be close to but less than unity.

Next, we consider the case of small Roche lobe size, i.e., 1.0 $R_\odot$. If we assume the composition of (0.63, 0.35, 0.02), no wind occurs for the region of $r_{\rm ph} < 1.0$ $R_\odot$. Then the accumulation ratio is the same as that for the solar composition. For the case of (0.109, 0.871, 0.02), a wind continues until the photospheric radius shrinks to 0.23 $R_\odot$. Therefore, the mass accumulation ratio becomes larger than that for the solar composition.

Ironically, the presence of wind mass loss increases the accumulation ratio when the Roche lobe size is small enough for the outer critical Roche lobe overflow to be effective. In the sequence of wind solutions the envelope mass is very sensitive to the surface temperature (i.e., the photospheric radius). In contrast to the wind solutions, the envelope mass in the static phase is almost constant on the plateau part in the H-R diagram. Therefore, the evolutionary time scale for the star to be moving in the H-R diagram, i.e., $dt/d(\log T_{\rm ph})$, is much longer in the wind phase than in the static phase. The mass accumulation in the static phase is determined mainly by the envelope mass with which the photospheric radius is just equal to the Roche lobe, because very little mass can be accumulated during the Roche lobe overflow phase. On the other hand, the mass accumulation in the wind phase is determined by the time scale of wind, which is much longer than that of the outer critical Roche lobe overflow. For example, the accumulation ratio is larger for a 1.3 $M_\odot$ white dwarf than for the other massive white dwarfs, as seen in Figure 6, because wind occurs in the region of $r_{\rm ph} < 10$ $R_\odot$ only for a 1.3 $M_\odot$ white dwarf.

ii) 1.0 $M_\odot$

When the Roche lobe size is 1.0 $R_\odot$, the accumulation ratio is calculated from the envelope mass at point E and the envelope mass at $r_{\rm ph} = 1.0$ $R_\odot$, which have been obtained in the previous subsection. Assuming the composition (0.73, 0.25, 0.02), we have obtained $\eta = 0.20$, 0.12, 0.073, and 0.054 for $\dot{m} = 1 \times 10^{-7}$, 1×10^{-8}, 1×10^{-9}, and 1×10^{-10} $M_\odot$ yr^{-1}, respectively. For the case of (0.5, 0.48, 0.02), η decreases to 0.18, 0.11, 0.063, and 0.047, respectively. For (0.109, 0.871, 0.02), $\eta = 0.13$, 0.084, 0.0487, and 0.036, respectively. We used the same ignition masses as for $X = 0.73$.

iii) 0.6 $M_\odot$

For a 0.6 $M_\odot$ white dwarf, the accumulation ratio is almost the same as for the solar composition. We assume that the Roche lobe size is 1.0 $R_\odot$. For the composition (0.5, 0.48, 0.02), $\eta = 0.31$, 0.20, and 0.15 for $\dot{m} = 10^{-7}$, 10^{-8}, and 10^{-9} $M_\odot$ yr^{-1}, respectively. For the solar composition (0.73, 0.25, 0.02), $\eta = 0.32$, 0.21, and 0.16, respectively. For the composition (0.109, 0.871, 0.02), η is very close to the value for the solar composition, i.e., 0.32, 0.21, and 0.16, respectively.

To summarize, the helium enhancement hardly affects the mass accumulation ratio when the Roche lobe size is relatively small and when the Roche lobe overflow is much more effective than that of the wind mass loss. The results in Figures 4–6 are not changed for the case of small Roche lobe sizes and relatively small white dwarf masses such as 0.6 $M_\odot$. For the case of large Roche lobe sizes and massive white dwarf masses such as 1.0 $M_\odot$, on the other hand, the mass accumulation ratio will certainly increase roughly by a factor of $0.73/X$ compared with that for the solar composition in Figures 4–6.

d) Accretion Rate and Composition of Nova Ejecta

As discussed in Paper I, we have not included the effect of hydrogen diffusion into the white dwarf matter. If this type of diffusion is effective, the accumulation ratio becomes smaller than our estimated values. This diffusion becomes effective for very low accretion rates such as $\sim 10^{-11}$ $M_\odot$ yr^{-1} (Paper I). So the mass accumulation may be negative for these low accretion rates because a part of the white dwarf matter is dredged up by convection and blown off the white dwarf (Prialnik 1986). Then we expect enhancement of the heavy elements in nova ejecta.

For relatively high accretion rates ($\dot{m} \gtrsim 10^{-9}$ $M_\odot$ yr^{-1}), on the other hand, the diffusion of hydrogen into the white dwarf matter is not effective, and then no part of the white dwarf

matter would be dredged up. Since a certain amount of the hydrogen-rich envelope mass still remains on the white dwarf surface after one cycle of the nova, we expect the solar CNO abundance in nova ejecta.

As for the helium enhancement, there are two possibilities: The first is the convective dredge-up of helium from the helium layer under the hydrogen burning zone. This is analogous to the dredge-up of carbon-oxygen material. This effect may occur even in relatively high accretion rates ($\dot{m} \gtrsim 1 \times 10^{-8}$ $M_\odot$ yr^{-1} for 1.3 $M_\odot$). Since the mass of the helium layer is about 100 times larger than that of the hydrogen layer, high helium content is expected once the convective mixing occurs. The second possibility comes from the inefficiency of the convection at the first phase of shell flash. At the rising phase, the helium processed by violent nuclear burning is carried by convection into the upper part of the envelope. If it is mixed completely with the envelope matter, the helium content near the burning zone will not increase so much. For example, the helium content, Y, increases by 0.1 for 1.3 $M_\odot$ and by 0.008 for 0.4 $M_\odot$. Here we have calculated the value from the relation $\Delta Y = GM_{\rm WD}/R_{\rm WD}\epsilon_{\rm H}$, where we assume that the hydrogen of $\Delta X = -\Delta Y$ is used to lift the envelope up against gravity. If the processed helium is not completely mixed with the upper part of the envelope, the inner part of the envelope would contain much more helium than the upper part. Then we can observe a high He/H ratio after the upper part of the envelope is removed by mass loss.

We expect the solar abundance of heavy elements for rapid accretion rates (i.e., recurrent novae). If the hydrogen shell flash is weak and the convection disappears at the very early phase, helium enhancement is possible. For the middle range of the accretion rates ($\dot{m} \sim 10^{-8}$ to 10^{-9} $M_\odot$ yr^{-1}), helium enhancement is also expected because of the diffusion of hydrogen into the helium layer. For the relatively low accretion rates (i.e., long recurrent period), the diffusion of hydrogen into the white dwarf core (carbon-oxygen or oxygen-neon-magnesium matter) is effective, so that we expect a high abundance of heavy elements.

These characteristics seem to be consistent with the observational features of novae. High CNO abundances have been observed in the ejecta of many fast novae. High helium abundances have been seen in slow novae (Truran and Livio 1986 and references therein). The recent observations of U Sco show that the ejecta of novae have the solar CNO abundance (Williams *et al.* 1981; Barlow *et al.* 1981). This object recently burst 8 yr after the previous outburst. Such a short recurrence period indicates high accretion rates. If we assume that this object has ever experienced many nova outbursts (i.e., the shell flash approaches the limit cycle; Sugimoto and Miyaji 1981), this 8 yr interval implies that the white dwarf is more massive than 1.3 $M_\odot$ and the accretion rate is higher than 5×10^{-8} $M_\odot$ yr^{-1} (Nariai and Nomoto 1979). Therefore, we expect the solar CNO abundance in the ejecta of U Sco. This is certainly ensured by the observations of Williams *et al.* (1981) and Barlow *et al.* (1981).

V. DISCUSSION

a) Comparison with Time-dependent Calculation

Recently Livio, Prialnik, and Regev (1989) computed weak hydrogen shell flashes on a 1.0 $M_\odot$ white dwarf for relatively high accretion rates. For the accretion rate of 1×10^{-8} $M_\odot$ yr^{-1}, a part of the envelope mass is lost from the system by wind. The envelope is in thermal equilibrium at the most expanded phase. Here, we mean by "thermal equilibrium" that the diffusive luminosity flux plus the advection flux is almost equal to the nuclear energy generation, i.e., $L_r + L_{\rm ad} \simeq L_n$. In a nova outburst, $L_{\rm ad}$ is much smaller than L_r. Livio, Prialnik, and Regev (1989) showed that L_r is almost equal to L_n. Thus, our assumption seems to be justified.

About half of the hydrogen-rich envelope mass is ejected during one nova cycle. In our terminology, the mass accumulation ratio is $\eta = 0.43$. This value is somewhat larger than our value, $\eta = 0.2$ (see Fig. 4). This discrepancy may come largely from Livio, Prialnik, and Regev's (1989) inconsistent initial model of the white dwarf. In our estimate we assumed that the white dwarf has already experienced so many shell flashes that the nova outburst has reached the limit cycle (see Sugimoto and Miyaji 1981). In such a situation, the white dwarf core is thermally balanced with the envelope, i.e., $L_r = 0$ at the core boundary. It seems that Livio, Prialnik, and Regev's (1989) initial model is somewhat hotter than that for the limit cycle. This implies that $L_r > 0$ at the bottom of the envelope, and then the ignition mass is smaller than that for the limit cycle. Their ignition mass is about one-half of that obtained by Nariai and Nomoto (1979). If they will follow shell flashes further, the white dwarf will become cooler and cooler. As a result, the shell flash will become much stronger than the first shell flash. Then we expect that much more envelope mass is ejected and the efficiency of accumulation decreases to as small as 0.2.

Livio, Prialnik, and Regev also computed shell flashes for the much higher accretion rate of 1×10^{-7} $M_\odot$ yr^{-1}. The shell flash is so weak that no envelope mass is ejected. The envelope expands up to 82 $R_\odot$. As they mentioned in the paper, the strength of the second flash is very different from that of the first one. The initial white dwarf model is far from the thermal equilibrium state of the limit cycle. Therefore we cannot compare this case directly with our results.

It should be stressed that, to obtain a reliable value of the mass accumulation ratio η by using time-dependent calculations, one must carefully choose the initial model of the white dwarf. Even if one chooses a thermally relaxed state for a given accretion rate, one must follow at least several shell flashes to see whether it has reached the limit cycle or not (e.g., Iben 1982). This is the best way to obtain a correct value of the mass accumulation ratio by using time-dependent calculations (see, e.g., Kato, Saio, and Hachisu 1989).

b) Radius of the White Dwarf

For simplicity, we used the Chandrasekhar radius with the mean molecular weight fixed to be $\mu_e = 2$. After the white dwarf suffers from many shell flashes, the white dwarf core will be thermally balanced with the envelope. Then the radius of the white dwarf depends not only on the white dwarf mass but also on the thermal state of the white dwarf. The ignition mass also depends on the thermal state and on the white dwarf mass. If we consider only the state on the limit cycle, which is realized after many shell flashes, the radius of the white dwarf and the ignition mass of the envelope are consistently determined. Nariai and Nomoto (1979) obtained the ignition masses in such states for various white dwarf masses and accretion rates. The radius of the white dwarf in thermal equilibrium obtained by Nariai and Nomoto (1979) is slightly smaller than the Chandrasekhar radius and depends weakly on the mass accretion rate. Moreover, the radius increases slightly during a nova

outburst, if the duration of the nova is very long compared with the thermal time scale of the white dwarf core. This may lead to a small overestimate of the mass accumulation ratio because the smaller radius tends to make a stronger wind for the same white dwarf mass. Even if we use the realistic values obtained by Nariai and Nomoto (1979), both the wind solutions and the static solutions are not so changed, because the difference between these two radii is very small (within a few percent). For the case of a 1.4 $M_\odot$ white dwarf, however, the Chandrasekhar radius is somewhat larger (about 20%) than the radius obtained by Nariai and Nomoto (1979), so that we did not calculate the accumulation ratio for the 1.4 $M_\odot$ white dwarf.

In order to examine the dependency of our wind solutions on the white dwarf radius, we have also constructed envelope models of very hot white dwarfs. The radius of such hot white dwarfs is rather larger ($\sim$20%–30%) than the Chandrasekhar radius. These hot white dwarfs may exist just after a red giant has evolved to a white dwarf. For such cases, our qualitative results—for example, the occurrence of the wind mass loss itself—are unchanged, but the detailed properties are slightly different. In general, the wind tends to be suppressed to some extent for the larger radii of the white dwarfs having the same mass. In the limiting case of very hot white dwarfs, optically thick wind occurs only for $M_{\rm WD} \geq 1.1\ M_\odot$. (Here we adopted the radius of the maximum energy generation of hydrogen burning in asymptotic giant branch stars [Iben 1982]. See § IV of Paper I for more detailed discussion on the properties of the wind on hot white dwarfs.) In usual cases of novae, however, the mass-accreting white dwarfs have already cooled down and the limit cycle of nova outburst has probably been established. Therefore, our assumption of the Chandrasekhar radius is a good approximation to the real situation of novae.

c) *Steady State Approximation*

We have obtained our wind solutions by assuming a steady state. This assumption must be confirmed by time-dependent calculations. Prialnik (1986) calculated a complete nova cycle by a hydrodynamical code. In her results, the steady state is realized during the wind phase after the maximum expansion: the mass flux $\dot{M} = 4\pi r^2 \rho v$ is constant throughout the envelope. To check the consistency between her results and ours, we have calculated the envelope for the same parameters as Prialnik's (1986). Assuming only the same critical point as in Figure 6 of Prialnik (1986), we have obtained the same envelope mass, the same photospheric radius, and the same mass-loss rate within the accuracy of the calculations. The radial velocity of the wind decreases rapidly near a point interior to the critical point. This point is also in good agreement with that in Prialnik's work. The detailed comparison will appear elsewhere. The reason for such good agreement is simply that the nuclear energy generation is almost equal to the luminosity, i.e., $L_n \simeq L_r$, and the envelope is in thermal equilibrium (that is, the radiative flux is almost constant in time until the star moves blueward in the H-R diagram to point E).

In our steady state solutions, the velocity does not vanish at the bottom of the envelope but is still finite (see Kato 1983). Also, the mass flux $4\pi r^2 \rho v$ does not vanish (because it is assumed to be constant throughout the envelope). This is not physical and, of course, is different from the solutions of time-dependent calculation, in which both the velocity and the mass flux decrease rapidly at the same point in the deep interior of the envelope. Nevertheless, our structures agree well with the structures of time-dependent calculations. This is because the envelope is almost hydrostatic in the deep interior where the velocity becomes very small. In this sense, the structure in the deep interior is determined independently of the mass flux itself.

In the case of helium novae, Kato, Saio, and Hachisu (1989) compared steady state solutions with time-dependent calculations. They computed the time-dependent calculations by using a hydrostatic Henyey code while they constructed the steady state wind solutions by the same method as in the present paper. Of course, they used the same opacity tables and the same physical parameters between these two numerical codes. Mass loss was included in their Henyey code by removing the matter outside the radius of 1.0 $R_\odot$, which was assumed to be the radius of the outer critical Roche lobe. They showed that the various features of the time-dependent calculation are consistent with those calculated from the steady state models. The interior structures of the time-dependent models are in good agreement with those in the steady state models.

In our steady wind models, mass-loss rate is obtained as an eigenvalue of the boundary-value problem. Therefore, its value itself is reliable. We usually use about 2000 mesh points and sometimes increase the mesh points to 20,000 as a numerical check. On the other hand, the mass-loss rates calculated from time-dependent models are not so accurate because the mass stripping in time-dependent codes is usually done by removing mesh points where the velocity exceeds the local escape velocity (e.g., Prialnik 1986). There are some problems in such a technique. For example, the photosphere is forced to be inside the region in which the velocity is equal to the local escape velocity. However, we have found some steady state models in which the photosphere is far outside the region where the velocity is equal to the local escape velocity (Kato 1983). Moreover, there is a large difference among the expansion speeds in the models computed by three different groups as discussed by Nariai, Nomoto, and Sugimoto (1980). (See also Sparks, Starrfield, and Truran 1978; Prialnik, Shara, and Shaviv 1979). We think that this problem is still not resolved numerically. In such a situation, our steady state models are useful to check the physical properties of the wind solutions.

d) *Helium Shell Flash and the Final Fate of a White Dwarf*

The long orbital period binary pulsars are believed to have evolved from low-mass X-ray binaries. Neutron stars in these binaries are believed to have formed through accretion-induced collapse of white dwarfs with shorter orbital periods (e.g., Taam and van den Heuvel 1986). Recently Chanmugam and Brecher (1987) suggested that the long orbital period binary pulsars formed from the accretion-induced collapse of white dwarfs in cataclysmic variables (see also Lipunov and Postnov 1985). However, the mass transfer rate from the companion in these systems is not so large and ranges from 10^{-11} to $1 \times 10^{-7}\ M_\odot\ {\rm yr}^{-1}$ (Patterson 1984). White dwarfs in these systems probably suffer many nova outbursts, and a significant part of the envelope mass is blown off. One important conclusion in this paper is that the probability of the accretion-induced collapse is very small once nova outbursts occur when the hydrogen-rich envelope has solar composition. The effect of CNO enhancement has not been clarified in this paper, however, because we have no proper ignition masses for enhanced CNO abundance.

Even if we can resolve the efficiency of mass accumulation in hydrogen novae, there still remains another problem: the effi-

ciency of mass accumulation in helium novae. When the mass accretion rate is higher than $2 \times 10^{-7}\ M_\odot\ \mathrm{yr}^{-1}$, no nova outburst occurs because the hydrogen shell burning is stable. Therefore, all the processed helium can be accreted by the white dwarf. When the helium envelope mass reaches a certain critical value, which depends on the mass accretion rate and the white dwarf mass, unstable helium shell burning ignites to trigger a novalike outburst (helium nova; see, e.g., Iben 1982 for such an example). Wind mass loss or the Roche lobe overflow occurs during helium nova outbursts, and a part of the accumulated helium envelope may be blown off. This effect considerably reduces the mass accumulation ratio, analogously to the hydrogen nova. In a separate paper (Kato, Saio, and Hachisu 1989), we have presented the sequence for a 1.3 $M_\odot$ white dwarf and show whether or not the white dwarf can grow to the Chandrasekhar limit.

The numerical calculations were carried out by Hitachi M-680H at the Computer Center of the University of Tokyo and by Fujitsu M-780/VP-200 at the Data Analysis Center of the Institute of Space and Astronautical Science. This research has been supported in part by the Grant-in-Aid for Scientific Research (63540196, 63740135, and 63302015) of the Japanese Ministry of Education, Science, and Culture.

REFERENCES

Barlow, M. J., *et al.* 1981, *M.N.R.A.S.*, **195**, 61.
Chanmugam, G., and Brecher, K. 1987, *Nature*, **329**, 696.
Finzi, A., and Wolf, R. A. 1971, *Astr. Ap.*, **11**, 418.
Fujimoto, M. Y. 1982*a*, *Ap. J.*, **257**, 752.
———. 1982*b*, *Ap. J.*, **257**, 767.
Iben, I., Jr. 1982, *Ap. J.*, **259**, 244.
Kato, M. 1983, *Pub. Astr. Soc. Japan*, **35**, 507.
———. 1985, *Pub. Astr. Soc. Japan*, **37**, 19.
Kato, M., and Hachisu, I. 1988, *Ap. J.*, **328**, 808 (Paper I).
Kato, M., Saio, H., and Hachisu, I. 1989, *Ap. J.*, **340**, 509.
Lipunov, V. M., and Postnov, K. A. 1985, *Astr. Ap.*, **144**, L13.
Livio, M., Prialnik, D., and Regev, O. 1989, *Ap. J.*, **341**, 299.
MacDonald, J. 1983, *Ap. J.*, **267**, 732.
McClintock, J., and Rappaport, S. A. 1985, in *Cataclysmic Variables and Low-Mass X-Ray Binaries*, ed. D. Q. Lamb and J. Patterson (Dordrecht: Reidel), p. 61.
Nariai, K., and Nomoto, K. 1979, in *Novae, Dwarf Novae and Other Cataclysmic Variables*, ed. H. M. van Horn and V. Weidemann (Rochester: University of Rochester Press), p. 525.
Nariai, K., Nomoto, K., and Sugimoto, D. 1980, *Pub. Astr. Soc. Japan*, **32**, 473.
Nomoto, K. 1987*a*, in *IAU Symposium 125, The Origin and Evolution of Neutron Stars*, ed. D. J. Helfand and J.-H. Huang (Dordrecht: Reidel), p. 282.
Nomoto, K. 1987*b*, in *Proc. 13th Texas Symposium on Relativistic Astrophysics*, ed. M. P. Ulmer (Singapore: World Scientific), p. 519.
Patterson, J. 1984, *Ap. J. Suppl.*, **54**, 443.
Prialnik, D. 1986, *Ap. J.*, **310**, 222.
Prialnik, D., Shara, M., and Shaviv, G. 1979, *Astr. Ap.*, **72**, 192.
Ruggles, C. L. N., and Bath, G. T. 1979, *Astr. Ap.*, **80**, 97.
Sawada, K., Hachisu, I., and Matsuda, T. 1984, *M.N.R.A.S.*, **206**, 673.
Sparks, W. M., Starrfield, S., and Truran, J. W. 1978, *Ap. J.*, **220**, 1063.
Starrfield, S., Sparks, W. M., and Truran, J. W. 1985, *Ap. J.*, **291**, 136.
———. 1986, *Ap. J. (Letters)*, **303**, L5.
Sugimoto, D., and Miyaji, S. 1981, in *IAU Symposium 93, Fundamental Problems in the Theory of Stellar Evolutions*, ed. D. Sugimoto, D. Q. Lamb, and D. N. Schramm (Dordrecht: Reidel), p. 191.
Taam, R. E., and van den Heuvel, E. P. 1986, *Ap. J.*, **305**, 235.
Truran, J. W., and Livio, M. 1986, *Ap. J.*, **308**, 721.
Truran, J. W., Livio, M., Hayes, J., Starrfield, S., and Sparks, W. M. 1988, *Ap. J.*, **324**, 345.
van den Heuvel, E. J. P. 1987, in *IAU Symposium 125, The Origin and Evolution of Neutron Stars*, ed. D. J. Helfand and J.-H. Huang (Dordrecht: Reidel), p. 393.
Williams, R. E., Sparks, W. M., Gallagher, J. S., Ney, E. P., Starrfield, S., and Truran, J. W. 1981, *Ap. J.*, **251**, 221.

IZUMI HACHISU: Department of Aeronautical Engineering, Kyoto University, Kyoto 606, Japan

MARIKO KATO: Department of Astronomy, Keio University, Kouhoku-ku, Yokohama 223, Japan